

# A Re-evaluation of Lamppost Deflection Data in the Buncefield Explosion

J. E. S. Venart, R. J. Rogers  
University of New Brunswick  
Fredericton, NB, Canada

## 1 Abstract

This paper presents finite element deformation studies of two types of lampposts found at Buncefield. The analyses use CJ blast loading based upon the posts being assumed to have been within the combustible cloud under a variety of blast and estimated negative wind conditions. The analyses and comparison to site photographs reveal discrepancies in the reported and the accepted, till now, assumed blast directions. These results, if true, suggest the necessity for a reevaluation of assumed ignition positions and blast formations in this event.

## 2 Background

On 11 December 2005, the Buncefield blast occurred. There were several detonative-like explosions as well as deflagrative events that resulted in severe damage to the surrounding area involving 23 fuel/oil storage tanks. A large amount of data was studied, catalogued and analysed; most of this summarized in [1-6], and others. The vapour cloud area was estimated to be around 120,000m<sup>2</sup> with the average cloud height between 2 to 3 m; in the Pump House Lagoon (PHL) area this was 4 to 5 m and involved somewhere in the order of two to three tonnes [3]. This gives a total volume of the cloud of 250,000 to 375,000m<sup>3</sup>. Evidence suggested the emergency pump house (PH) as one possible ignition source [1]; other suggestions in addition involved vehicle remote keyless (RKE) alarms [2-4] activated by the PH explosion and a hypothesised fire-ball.

Detailed CFD modelling reported in [1] of the area immediately surrounding the emergency pump house (PH) suggested that if ignition occurred there the trees and undergrowth surrounding may have allowed flame acceleration from a prior interior PH explosion to run-up to several hundred m/s north-west along Cherry Tree Lane to DDT [1] at its intersection with Buncefield Lane, and then south down Buncefield Lane, and thus the progression of a single detonation front, from this source, within the vapour cloud. CCTV footage however showed that the explosive and illumination events took place over a period greater than three seconds [1] to finally end at the brick wall separating the NG and 3Com buildings car-parks; turning W and finally ending at the flammable cloud edge located just W of the auxiliary generator and the SE corner of the NG Building.

It was noted that many vehicles located in the NG and Fuji Building car-parks, within the combustible limits of the vapour cloud, were crushed, windows broken and moved/slewed E: Many with deflated and debeaded tyres [1, 5, 6]. After the explosions most vehicles were still aligned N-S with their bonnets to the N though slewed E. Blast experiments carried out by the UK MoD using high explosive charges indicated comparable vehicle side on damage and tyre deflation/debeading at levels that would suggest hydrocarbon gas cloud detonations [1]. Experiments and analysis by Haider et al [5] indicated that the minimum necessary average over-pressure to debead and deflate tyres was about 0.8MPa, also suggesting detonative overpressures in parts of the cloud – the CJ detonative pressure for Butane, a major constituent of the fuel spilled, is 1.83MPa [7]. CCTV video analyses, photography, and simple models for vehicle blast damage and sliding [2] under the influence of an idealized blast [8] and its resulting negative phase [2] concluded that the statement made in [1, p31], that *“the most likely scenario ...was a deflagration outside the emergency pump house that changed into a detonation due to flame acceleration in the undergrowth and trees along Three Cherry Trees Lane”*, is possibly incorrect due to inconsistencies in interpretations of directional indicators and the apparent evidence from the vehicles noted above.

The present paper follows that of [2, 4], to examine further CJ detonative blast analyses of lamppost deformation and breakage using analyses similar to that used earlier [2]. In a preliminary examination of directional displacements and crushing evidence it was noted [3] that, if subjected to detonative loading within the cloud, the base of lampposts would deform in the direction of the blast despite significant negative phase loading. A somewhat similar analysis, though only subject to blast [10] noted comparable results. This is at variance with some analyses by Atkinson et al [11] and Johnson [12].

### 3 Lamppost blast loading and deformation

Venart and Rogers [4] in their analyses of CCTV records from the RO and Furnel Buildings noted that the explosion development was very complex. That analysis supported a hypothesis consisting of two major deflagrative and two, near simultaneous, detonative events. The HSE report rr718 [1], and many others, e.g. [11], however, suggested DDT and a continuously developing event over an observed CCTV period of greater than 3.66 seconds! Directional evidence in the form the deformation and snapping off and bending of lampposts, fence posts, CCTV masts, trees, displacement of vehicles, etc., assumed representative of the negative phase pressure loading, was used in support of this conclusion.

There were, however, many inconsistencies in the observed data for the lampposts and vehicles. Most lampposts in the car park directly E of the NG Building appeared to be vertical and not deformed – though many had been abraded by dust and grit on their bases. However many lampposts were snapped off or buckled most, with bases and poles pointing east or north east – some confusingly so, Figures 1(a, b).

For example Figure 1(a) shows a fractured lamppost felled to the north east (with another to the west behind it in the Fuji car park felled to the east). Here the western Buncefield Lane perimeter fence between the Fuji car park and Buncefield Lane appears to have been displaced upwards before the post was felled by blast. This blast, speculated to originate from the N side of shrubs/fencing must have taken place after an updraft, possibly caused by a rising fireball from ignition of the richer fuel in the lagoon [2], allowing the fence to drop down over top of the now already blast felled lamppost.

In an attempt to understand this behaviour, several lamppost FE (Finite Element) models were constructed and subjected to a variety of blast loadings using the ideal blast model taken from Venart and Rogers [4]. The Abaqus/Explicit FE code v6.14-1[16] was used.

#### 4 Lamppost models

As hypothesized here a lamppost might have experienced two opposite load steps due to over-pressure events. The first and positive load step acting toward the east was taken as 5.4ms in duration (Venart and Rogers [2] and in [1] as given by Fluid Gravity (FG) for the various pressures and velocities of a pancake shaped centrally ignited symmetrical detonation model.) This positive over-pressure was assumed to decrease linearly with time according to FG. The pressure acting on the lamppost components during this load step is the dynamic pressure  $q$  given by  $5/2 p^2/(7p_0+p)$  where  $p$  is the time dependent blast pressure decreasing from 1.8MPa (the detonation pressure of Butane) behind the shock front with  $p_0$  atmospheric pressure; the density  $\rho$  behind the shock front given by  $\rho_0[(7+6p/p_0)/(7+p/p_0)]$ ; with the corresponding particle, or wind, velocity  $V$  given as  $(5p/7p_0) \cdot c_0/(1+6p/7p_0)^{1/2}$ , with  $c_0$  the ambient speed of sound (ahead of the shock front). All properties are determined based upon the Rankine-Hugoniot conditions for a true (or ideal) shock wave [8].

The second load step considered an air velocity of 300m/s in the opposite direction to blast. The first ramp was taken as linear from zero over 20ms, constant for 120ms at 300m/s and then linear to zero over 20ms [1]. The drag pressure on the lamppost is given by  $-1/2 C_D \rho V^2$  where  $C_D=1$  as consistent with the negative phase though somewhat reduced to take into account side relief since the cloud in reality was three dimensional not two dimensional as in the FG model [1]. The negative drag pressure acts on the projected area of the post which is already in motion and deformed. The relative velocity of the lamppost is neglected; since the peak lamppost velocity is approximately 90 m/s, this is not a major simplification. Following these two load steps would be a period of free movement until the lamppost and its components come to rest. A variety of loads were assumed ranging from 75 to 100 percent of the full detonative and negative pressure phases.

The first lamppost analysed is referred to as type A and was similar to the one shown in Figure 1(a). Its assumed components (length units converted to m) consisted of (a) main pole: 24 ft. long 3 in. schedule 40 steel pipe, (b) base: 4 ft. long 6 in. schedule 40 steel pipe, (c) connecting cone, (d) connecting flange inside base: at 24 in. from bottom, between base pipe and main pole, and (e) top box: 18 in. by 36 in. by 4 in. high.

The material was taken as steel [17, 18] with a yield strength of 345 MPa (50 ksi) and used the following plastic strain/stress (MPa) hardening values: 0, 345; 0.01, 375; 0.03, 400; 0.05, 410. Ductile damage parameters were assumed. The mesh of linear shell elements had 36 nodes around the circumferences. All joints were “*tied*” except between lamp box and pole where a friction interaction was used. The loading consisted of a gravity load applied gradually for 0.05 s with damping to avoid numerical waves; the pressure loads (general traction along a horizontal direction) on the pipe surface and box ends. The positive load peak was 3.24MPa decreasing to 0 in 5ms; the negative load peak was -57.2kPa. The solution used time steps of 0.5 to 0.8 $\mu$ s.

Figure 2(a) shows the slight deformation after the positive load phase and Figure 2(b) shows the configuration at  $t=1.2$ s. The simulated system is not quite at rest and further vertical settling will occur. The base post shows a permanent lean in the direction of the positive

pressure. The pole snapped at the base-pole connection and lamp box landed to the east of the base post, consistent with the actual lamppost shown in Figure 1(a).

A second lamppost based upon that shown in Figure 1(b) was also modelled. This tapered lamppost, called Type B, was located just south of the eastern corner of the Fuji Building. Blast is again presumed to originate from W going E. This lamppost and simulated lamp housing were modelled using linear shell elements of the same steel and hardening characteristics as for the Type A model. The above ground pole is 8m long and tapers from 0.2m to 0.1m mean diameter. Its 4mm thickness provides the 8m pole with a weight comparable to a commercial lamppost [17]. The access cut-out is centred at 0.75m from ground on the negative Z-face (S). The pole base is 0.2m in diameter and extends 1m into the soil before it is rigidly fixed. A 1m long tapered tube extends at 45degrees from the top of the pole and is attached to a short horizontal tube and a body of revolution that represents the lamp. The soil model uses a Drucker-Prager plasticity model based on an Abaqus oil well example [16]. The pressure load was a general traction in the negative X-direction (blast wind from W to E). Time steps were about 0.2 $\mu$ s.

The simulation results for the Type B lamppost for the 100 percent loading are shown in Figure 3. Reduced loading at 75 percent loads, for both positive and negative phases, left the pole only bent; 75 percent positive loading and 100 percent negative loading caused the pole to bend to the E during the positive and negative loadings, but finally buckle and fall to the W; however its base was still left tilted E due to the original positive phase load.

## 5 Discussion and Conclusions

Most lampposts in the car park directly E of the NG Building appeared to be *vertical* and *not* deformed and thus have not been exposed to large positive or negative pressure loads. Lampposts, at the S and E edges of the Fuji car-park were severely deformed, bent with some collapsed or snapped/fractured. Most of these were pointing E or NE. Simulations of the response of this style of lamppost (Type A) to positive and negative phase pressure pulses (consistent with an eastward or northward moving CJ blast, including its resulting negative wind loading) indicate that the base would incline to the E or N by the initial blast, fracture at the joint with the base post and then the broken section land E or N of its base post. From these simulations it can be concluded that the photographs of the Type A lamp pole assembly analyses correctly identify that these poles were struck by detonation blasts originating from the W and S.

In the case of the Type B lamppost model, the tapered pole with side cut-out, the loading response was sensitive to direction and positioning of both the cut-out and the positioning of the offset lamp housing relative to the assumed CJ blast direction. In order to replicate the collapse mode noted in Figure 1(b), the pole had to be buried in a simulated surrounding soil. The case with a S exposure of the cut-out and N extension of the lamp arm under a CJ blast originating from the W replicated quite well the observed failure for the lamppost located near the SE corner of the Fuji building, Figure 1(b) and Figure 3.

The success of this modelling attempt should call for a reassessment of the currently accepted source of blast, further more detailed investigation as to the methods of ignition, and blast sustainability of what has been shown to be a very long lasting and complex combustion event. Video records of the simulation results can be provided as supplemental material.

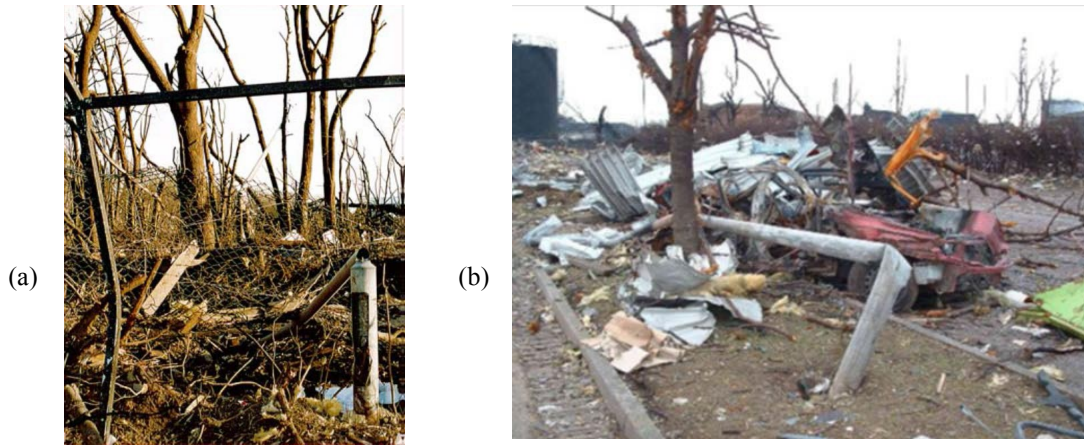


Figure 1. (a) Type A light pole on the W side of Buncefield Lane opposite the eastern edge of the Fuji Building indicating a felled E direction. The fence appears overtop the already fallen light-pole [9]. (b) View from the W of lamp pole Type B very near the S-E corner of the Fuji Building. The lamppost has been hit by blast, buckled and felled E [9].

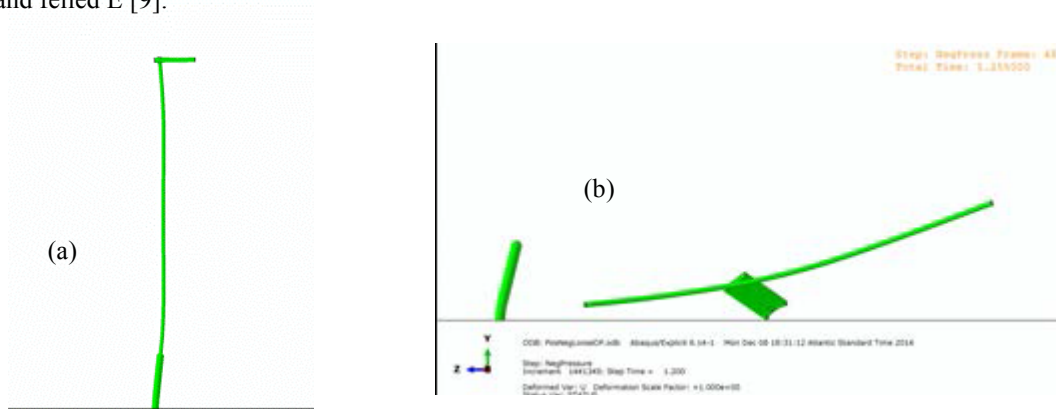


Figure 2. Type A lamppost: (a) At end of positive phase loading,  $t=0.005s$ . (b) At  $t=1.2s$ .

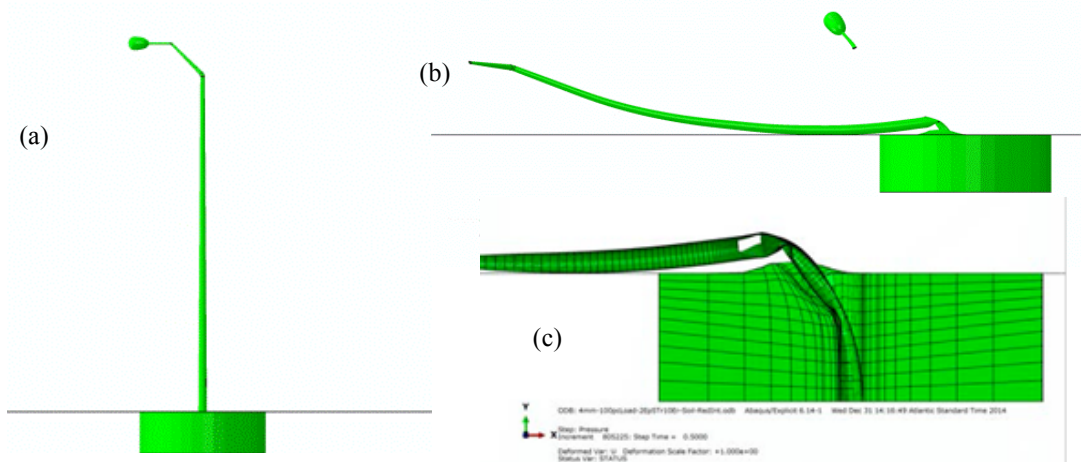


Figure 3. Type B lamppost (a) Initial condition. (b) End of simulation for 100 % blast and negative phase loading. Blast direction from right to left. (c) Close up of buckled, 100% loaded Type B lamppost; blast direction from right to left. Note soil deformation and compare to Figure 1(b).

## References

- [1] Steel Construction Institute (2009). “Buncefield Explosion Mechanism; Phase 1,” Vol. 1 and 2, Health and Safety Executive (HSE), rr718, December, 226 p.
- [2] Venart JES & Rogers RJ (2011). Buncefield: Questions on the development, progression, and severity of the explosion. In *Fire and Explosion Hazards: 6th Int. Seminar, Leeds* (eds D Bradley, G Makhviladze & V Molkov), pp. 52--65. Singapore: Research Publishing.
- [3] Venart J (2011). Buncefield: reconciliation of evidence with mechanisms of blast, ICDERS 23rd Int'l Colloquium on the Dynamics of Explosions and Reactive Systems, Irvine CA, July 24—29.
- [4] Venart JES, Rogers RJ (2011). The Buncefield Explosion: Vapour Cloud Dispersion and Other Observations, Proc. IChemE Hazards XXII, Liverpool, April
- [5] Haider MF, Rogers RJ, Venart, JES (2011). External Pressures required to debeat tyres, In *Fire and Explosion Hazards: 6th Int. Seminar, Leeds* (eds D Bradley, G Makhviladze & V Molkov), pp. 66-75. Singapore: Research Publishing.
- [6] Bradley D, Chamberlain GA, Drysdale DD, Large vapour cloud explosions, with particular reference to that at Buncefield, *Phil. Trans. R. Soc. A* 2012 370,544-566, doi: 10.1098/rsta.2011.0419
- [7] Vasil'ev AA (2009). “Detonation Properties of Saturated Hydrocarbons”, *Combustion, Explosion, and Shock Waves*: 45, 6, pp. 708–715.
- [8] Glasstone S, Dolan PJ (1977). “The Effects of Nuclear Weapons,” United States Department of Defence and the Energy Research and Development Administration, Washington, DC.
- [9] Atkinson G (2012). “Buncefield Archive CD + extended CCTV video files”, 27/04.
- [10] van Netten AA, Dewey JM (1997). A study of blast loading on cantilevers, *Shock Waves* 7: 175-190.
- [11] Atkinson G, Cuso L, Painter D, Tam V (2009). Interpretation of overpressure markers and directional indicators in full-scale deflagrations and detonations, IChemE Symp Series 155, Hazards XXI, 500-506.
- [12] Johnson DM (2010). The potential for vapour cloud explosions the Lessons from the Buncefield accident, *Journal of Loss Prevention in the Process Industries*, doi:10.1016/j.jlp.2010.06.011
- [13] Health and Safety Executive (1975). ‘The Flixborough Disaster : Report of the Court of Inquiry’, HMSO, ISBN 0113610750.
- [14] Roberts AF, Pritchard DK (1982). Blast effect from unconfined vapour cloud explosions, *J. Occupational Accidents* 3\_1982. 231–247.
- [15] Venart JES (2004). *Flixborough: the explosion and its aftermath*, Trans. IChemE Part B, *Process Safety and Environmental Protection*: 2004, 82 (B2), pp 105-127.
- [16] Abaqus Analysis User's Manual v6.14-1 (2014). Online Documentation, Dassault Systemes Simulia Corp., Providence, RI, USA.
- [17] Dynapole, TRS series, tech. details (2004). <http://www.dynapole.com/gifs/products/trs.pdf>
- [18] Schmidt LC, Lu JP, Morgan PR (1989). “The influence on steel tubular strut load capacity of strain hardening, strain aging and Bauschinger effect”, *J. Construction Steel Research* 14: 107-119.